



ELSEVIER

Nuclear Instruments and Methods in Physics Research A 466 (2001) 527–537

---

**NUCLEAR  
INSTRUMENTS  
& METHODS  
IN PHYSICS  
RESEARCH**  
Section A

---

www.elsevier.com/locate/nima

# The stabilization of a positron lifetime spectrometer with a high-accuracy time reference

J. Nissilä\*, M. Karppinen, K. Rytsölä, J. Oila, K. Saarinen, P. Hautojärvi

*Laboratory of Physics, Helsinki University of Technology, FIN-02015 HUT, Espoo, Finland*

Received 14 November 2000; accepted 16 November 2000

---

## Abstract

A high-accuracy time reference for a fast coincidence apparatus using scintillation detectors is constructed. The reference peak is created by feeding fast light pulses from a light-emitting diode along two optical fibers of different lengths onto the photomultipliers. The peak can serve as a basis of digital hardware or software stabilization. A particular advantage of the system is that the accuracy of drift detection can be enhanced notably by using a high frequency in the reference peak. In a one-week-long test measurement with a positron lifetime spectrometer, drifts of 12 ps were reduced below a level of 0.5 ps with hardware stabilization. © 2001 Elsevier Science B.V. All rights reserved.

*PACS:* 78.70.Bj; 07.85.Nc; 29.30.Kv

*Keywords:* Fast coincidence apparatus; Digital stabilization; Positron lifetime spectrometer

---

## 1. Introduction

Positron annihilation spectroscopy is a technique that can be used to probe the electronic and defect structure of solids [1]. Positrons annihilate with electrons leading to the emission of two 511-keV  $\gamma$ -quanta. Both the positron lifetime and the energy spectrum of the annihilation radiation yield invaluable information about the electronic environment in which the annihilation takes place. As an example, positrons are able to distinguish unambiguously vacancy-type defects from other point defects since the positron lifetime increases due to the reduced electron density in the vacancy.

Positron lifetime spectroscopy is a method which has provided a lot of information about the structure and concentration of open-volume defects in various materials during the last decades [1].

Conventionally, the positron lifetime is measured as a time difference between two photons. The birth of the positron is marked by the emission of a  $\gamma$ -quantum from the daughter nucleus of the positron emitter (usually  $^{22}\text{Na}$ ), and the annihilation is revealed by the annihilation  $\gamma$ -quanta. Fast scintillation detectors are used for the detection of the photons since the lifetime is typically only some hundreds of picoseconds. Drifts in the detectors and electronics are usually of the order of tens of picoseconds in a week, which worsens the quality of the data. An improvement in the stability of the lifetime

---

\*Corresponding author. Tel.: +358-9-451-5802; fax: +358-9-451-3116.

E-mail addresses: jaani.nissila@hut.fi (J. Nissilä).

spectrometer is desirable due to a number of reasons. For example, if the time zero were stable, changes in the average lifetime could be analyzed simply based on the movements of the centroids of the spectra. Thereby uncertainties related to multiexponential fitting could be eliminated. An improvement in accuracy by acquiring high-statistics data would also be attainable. As far as we know, no stabilized lifetime spectrometers are currently in routine use.

A couple of suggestions to improve the stability of lifetime data have been given in the literature. Crisp et al. reported a system in which they collected two spectra simultaneously: a symmetrical lifetime spectrum and a conventional lifetime spectrum in two different segments of the memory of the multichannel analyzer [2]. The symmetrical spectrum was used as a basis for the stabilization of the time zero. Besides digital stabilization of the spectra they also stabilized the temperature of the apparatus. As a result, they achieved an order-of-magnitude improvement in the stability of the time zero. Dias and coworkers collected statistically adequate data in parts and developed a software algorithm to detect the drifts and move the partial spectra accordingly [3]. They also reported a considerable improvement in the stability of the time zero and in the quality of the fits. A limitation to both of these methods is posed by the statistical reliability of the corrections: they are based on the slowly accumulating lifetime data and therefore fast drifts cannot be observed.

In this work, we have developed an apparatus which produces an artificial time reference peak in the lifetime spectrum. This peak serves as the basis of corrections for a digitally stabilized multichannel analyzer (MCA). The reference peak is created by guiding light pulses from a single light-emitting diode (LED) via two optical fibers of different lengths to the photomultipliers. The transit time difference in the optical fibers is very stable and the resulting reference peak enables drifts in all components of the spectrometer to be observed and corrected. A considerable advantage of our scheme is the possibility to attain a sufficient statistical accuracy to observe even the fastest drifts by simply increasing the flashing frequency of the LED.

With the apparatus described in this paper the stability of the time zero of the lifetime spectra was improved considerably. In a one-week-long set of test measurements the drift of the centroids was reduced from 12 ps so that the standard deviation (STDV) of the stabilized centroids was close to the statistical accuracy limit of 0.3 ps. The time reference scheme presented here is applicable to all kinds of fast coincidence apparatuses with scintillation detectors.

## 2. Time drifts in a positron lifetime spectrometer

The conventional positron lifetime system is a fast coincidence spectrometer which consists of two scintillation detectors, two timing discriminators, a time-to-amplitude converter (TAC) and a multichannel analyzer (MCA) (part of Fig. 1). One of the detector–discriminator combinations (start)

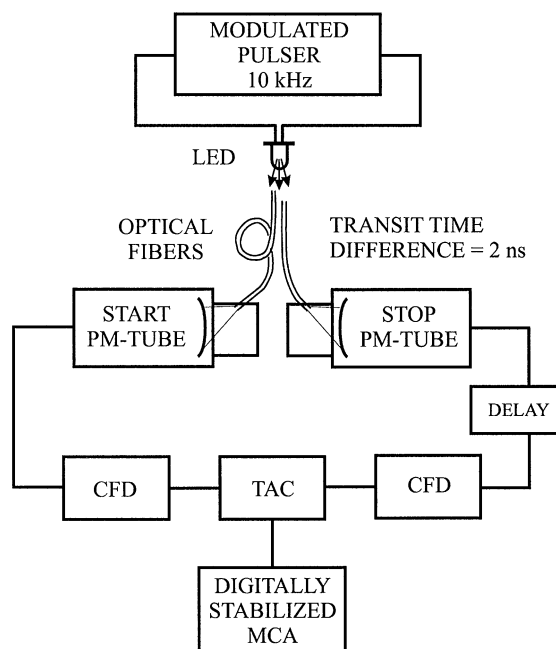


Fig. 1. A schematic diagram of the digitally stabilized positron lifetime spectrometer. The stabilization is based on an artificial time reference peak created by a flashing LED which emits light pulses along two optical fibers of different lengths onto the photomultipliers.

is set to observe the 1.28 MeV  $\gamma$ -quanta resulting from the decay of  $^{22}\text{Na}$  and the other (stop) to detect the annihilation  $\gamma$ -quanta (511 keV). Plastic scintillators are most common in the detectors because they are easy to use and their timing properties are excellent. Due to the low density of the material the pulse height spectrum resulting from  $\gamma$ -ray interactions includes only the Compton continuum (no full-energy peak). The energy windows (the spectra of pulses used in the measurement) are set at the Compton edges and they are typically 20–50% wide.

In our test spectrometer we used cylindrical ZL-236 scintillators coated with white diffusely reflecting paint. The crystal sizes were  $\phi 40 \times 25 \text{ mm}^3$  in start and  $\phi 30 \times 20 \text{ mm}^3$  in stop. As photomultipliers (PM) we used Philips XP2020 tubes. The constant-fraction discriminators (CFD) were Ortec 583's, the time-to-amplitude converter was Ortec 566 and the digitally stabilized multi-channel analyzer was Ortec 919. We used 45% energy windows and the time resolution in a positron lifetime measurement was 250 ps (full width at half maximum, FWHM).

The stabilization performed by the Ortec 919 MCA is based on observations of the movements of one or two reference peaks, and corresponding corrective actions. There are two alternative stabilization methods in the Ortec 919: the point- and the Gauss-mode stabilization. In the point mode the reference peak is divided into two neighboring sections. If a pulse comes to the lower section the offset (or the gain) of the stabilizer amplifier is increased immediately by an incremental amount, and vice versa. In the Gauss mode, counts coming into the reference peak region are collected to a separate buffer. The number of counts in the buffer is checked once a minute and after a preselected number of counts has been accumulated, a Gaussian function is fitted to the data. Based on the fitted centroid a correction is done for the pulses coming during the next period. The magnitude of the correction equals that multiple of 0.125 ps (25  $\mu\text{V}$ ) which corresponds closest to the difference between the fitted centroid and the nominal position. After each correction the data in the buffer are erased.

Instabilities in the lifetime spectrometer can be divided into two groups: the channel width can change (drift in gain) and the time zero can move. The time zero drift can originate in all the components whereas gain changes are possible only in the TAC and the MCA. Drift in time zero means that the magnitude of the shift in channels in the MCA is independent of the time interval observed. Drift in gain, again, leads to shifts which increase with increasing time interval.

The drifts could be ideally corrected by using two reference peaks, one at the beginning of the spectrum to detect zero drifts and the other at the end for changes in the gain. This method is called two-point stabilization. In this work we use only one reference peak located very near the lifetime spectrum (one-point stabilization). The stabilizer is used in the zero-stabilization mode, i.e. the stabilizer performs corrections by changing the offset voltage in the input amplifier of the ADC (stabilizer amplifier). The choice of using this method is based on a hypothesis that most of the drifts are related to the photomultipliers and the CFDs [4]. Changes in the operating conditions of these parts of the spectrometer can only lead to zero drifts. For example, if the supply voltage over the PM-tubes changes, the transit times and the pulse heights change. These both result in a change of the time interval between the timing signals from the CFDs. This drift is equal for all intervals and is thus effectively zero-point drift. The reference peak located next to the lifetime spectrum follows these drifts accurately. By setting the reference peak near the lifetime spectrum instead of in the beginning of the whole spectrum the possible drifts in gain are also partially corrected.

### 3. A high-accuracy time reference for fast coincidence spectrometers

#### 3.1. Light source, optical fibers and mounting

To stabilize drifts in all the components of the spectrometer, the reference time difference signal has to be produced at the point of light pulses

entering the photomultiplier tubes. An essential design criterion of the system is, of course, that the reference peak must not move on its own, i.e. due to the instability of the apparatus creating the peak. All the shifts in its position must be fully correlated with drifts to which the real lifetime spectrum is exposed to.

Lindskog and Svensson have reported a digitally stabilized coincidence spectrometer operated in the two-point stabilization mode [5]. The reference peaks are produced by two LEDs flashing near the PM-tube photocathodes with suitable time delays between the light pulses. They use a single pulser to drive the LEDs and the proper time delays are realized with electrical delay lines. They obtain reference peaks with  $\text{FWHM} = 1$  ns and are able to reduce the centroid shifts from tens of picoseconds to below 10 ps with stabilization.

Our goal was to reach an accuracy better than a picosecond. Therefore, we use only a single LED, which feeds light pulses into two optical fibers of different lengths. The other ends of the fibers are mounted into the scintillators in front of the photocathodes (Fig. 1). With this solution we get rid of possible problems related to the individual operational changes in LEDs (e.g. aging) and the temperature sensitivity of the transit time of passive delay lines.

An ultrabright fast 592-nm LED (model HP HLMA-CLOO) was selected as the light source of the apparatus. The maximum luminous intensity of this LED is 3 Cd which was found to be high enough for easy adjustment of the pulse heights. A further advantage of this LED is that the light spread from it is only  $7^\circ$  which means that all the light travels in the multimode fiber without attenuation.

The transit time difference of 2 ns in the fibers (40 cm in length) results in a reference peak next to the positron lifetime spectrum (Fig. 2). To minimize the sensitivity of the transit time difference on ambient conditions we use a quartz multimode fiber (type 3 M FT-1.0-LMT) whose temperature expansion coefficient is of the order of  $10^{-6}$  1/K. A small hole is drilled on the scintillator edge in which the end of the fiber is attached with optical grease. The mounting position and angle were selected such that the light spot covers nearly the

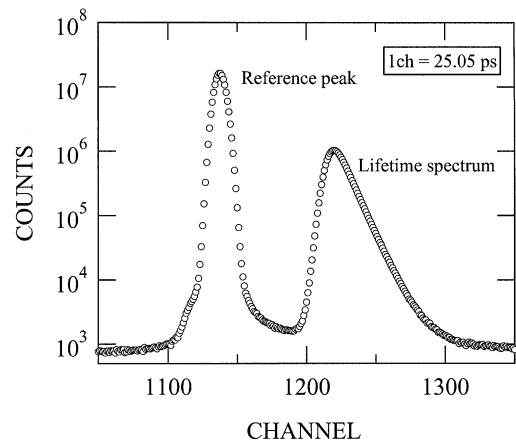


Fig. 2. The reference peak and a positron lifetime spectrum measured in Si. The nonGaussian tails around the reference peak are due to pulse pile-up between the LED pulses and  $\gamma$ -pulses. (For the shape of the reference peak in the absence of a  $\gamma$ -source, see Fig. 5).

whole photocathode. The fine adjustment of the light levels for the start and stop detectors is done by moving the fibers relative to the LED. The mechanical attachments of the fibers must be very stable since a change of only 0.3 mm in the length of the optical path from the LED to the photomultiplier leads to a shift of 1 ps in the reference peak position.

### 3.2. Modulated pulser

To drive the LED we designed a modulated pulser depicted in Fig. 3. It consists of three different operational units, a fast pulser, a triggering circuit and a nonlinear amplifier. In addition, a conventional signal generator is needed. In brief, the fast pulser is actually a circuit which drives a very short ( $\sim 10$  ns) current pulse through the LED. The triggering unit starts the operation of the fast pulser and determines the flashing frequency. The amplitude spectrum of the light pulses is determined by the nonlinear amplifier, the input of which is a triangular wave riding on a negative bias voltage. In the following we explain in detail the operation and ideas behind the modulated pulser.

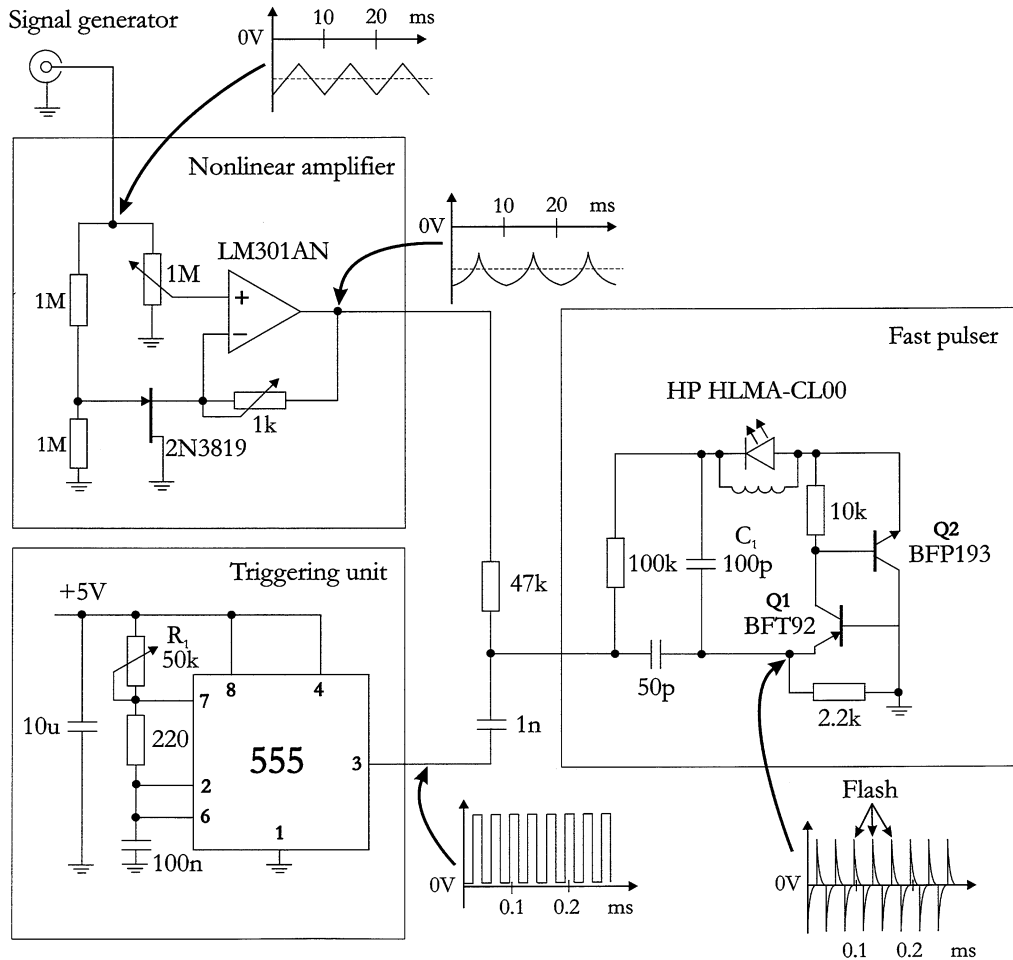


Fig. 3. The circuit diagram of the modulated pulser used to drive the LED. To produce the required continuous distribution of pulse amplitudes (see Fig. 4) the circuit requires as input a triangular wave riding on a negative bias from a signal generator. The input voltage is adjusted together with the optical fiber positions such that the LED pulse height distributions cover the energy windows properly (see Fig. 4). Notice that the time scales in the inserts describing the waveforms are different in case of the nonlinear amplifier and the triggering circuit.

The timing discriminators are optimized for pulses originating from  $\gamma$ -quanta. To obtain the narrowest possible reference peak we aimed at generating similar pulses also from the LED. This is achieved by using a fast pulser presented by Kapustinsky et al. [6] to drive the LED (see Fig. 3 for the circuit). The amplitude of the light pulse is determined by the voltage to which the 100 pF capacitor  $C_1$  is charged before the pulser is externally triggered. When a pulse arrives from the triggering unit the transistor Q1 starts con-

ducting which leads to the opening Q2. This complementary pair of transistors provides a low-impedance path for the capacitor  $C_1$  to discharge through the LED. The inductor across the LED shortens the pulse to the desired length.

The light output of the LED depends strongly both on its supply voltage and temperature. On the other hand, it is known that the timing instant in a CFD depends on the pulse amplitude due to the so-called walk effect [7,8]. Therefore, even normally observed small changes in the temperature

of the LED and the driving voltage result in changes in the timing instants and thereby shifts in the reference peak position. We observed shifts of the order of 2.5 ps/K and 2 ps/10 mV.

This problem can be solved by producing even distributions of LED pulse amplitudes, which cover the whole energy windows of the CFDs (and extend slightly beyond the edges). Then, irrespective of changes in the ambient conditions, the LED pulse height distributions inside the windows are always the same (i.e. flat). Using a simple triangular waveform riding on a negative offset voltage to charge the capacitor  $C_1$  leads to a distribution whose intensity decreases notably with increasing pulse amplitude. This is evidently due to the nonlinear current–voltage relationship of the LED. With uneven pulse height distributions, changes in the LED-related conditions lead to drifts of the reference peak. Flat distributions can be produced by modifying the triangular wave with a nonlinear amplifier which counteracts the nonlinearity of the distributions obtained with a pure triangular wave. The idea of the nonlinear amplifier is simply to increase the fraction of time that the voltage stays at larger negative values. Then, more high-amplitude pulses are created at the expense of lower ones.

A simple way of realizing a nonlinear amplifier is to use a JFET as a voltage controlled resistor in the feedback loop of an operational amplifier (see Fig. 3). The output voltage of the amplifier is of the form  $U_{\text{OUT}} = GU_{\text{IN}} = (A + BU_{\text{IN}})U_{\text{IN}}$ . The constants  $A$  and  $B$  depend on the resistances in the circuit and the properties of the JFET [9]. The waveform coming out of the nonlinear amplifier is schematically illustrated in Fig. 3.

For triggering the fast pulser we use a simple oscillator circuit (see Fig. 3) producing a square wave. Due to the capacitive coupling the voltage at the emitter of the transistor Q1 consists of positive and negative spikes as seen in Fig. 3. The operation of the fast pulser starts at the leading edge of the positive part. The flashing frequency is determined by the value of  $R_1$ . Its selection is discussed in Sections 3.3 and 4.1.

As explained above, different LED pulse amplitudes lead to different reference peak positions due to the walk of the discriminators. Even when using

the modulated pulser, one has to take this into account as follows. To enable a reliable correction of the drifts by the stabilizer, the whole energy window must be swept through many times ( $> 100$ ) within the period that appreciable drift occurs. If the Gauss mode of Ortec 919 is used, a further condition is that a large number of complete cycles ( $> 100$ ) have to be run during the time that counts are collected to the stabilization buffer (an integer multiple of 60 s). Thereby the fraction of counts in the buffer acquired during an incomplete sweep over the window, leading to walk and an inaccurate correction, is negligible. On the other hand, to produce an even and sufficiently dense distribution of different pulse amplitudes, the sweeping frequency should be at least an order of magnitude lower than the flashing frequency. In this work the sweeping frequency was around 100 Hz.

### 3.3. Performance

The LED pulse height distributions from the start and stop detectors, obtained by using the modulated pulser, are shown in the lower part of Fig. 4. In the upper part, we show the pulse height spectrum resulting from the  $\gamma$ -rays emitted by a  $^{22}\text{Na}$  source (consisting of the Compton continua of 511 keV and 1.28 MeV  $\gamma$ -rays). The vertical dashed lines depict the typical limits of the energy windows. To adjust the LED pulse height spectra around the energy windows as shown, the fiber ends connected to the start and stop detectors were set at distances of 2 and 4 mm from the active region of the LED, respectively.

By using the modulated pulser instead of a simple constant-voltage-driven LED the sensitivity of the reference peak to changes in the average driving voltage is reduced by a factor of 250 to a level of 1 ps/V. Thus, a stability of some tens of millivolts in the negative offset voltage, which is easily reached with commercial signal generators, is sufficient to hold the reference peak stable enough for our purposes. A slight problem with our apparatus is the remaining sensitivity on the LED temperature, 0.5 ps/K. If needed, this problem can be solved by stabilizing the temperature of the LED surroundings.

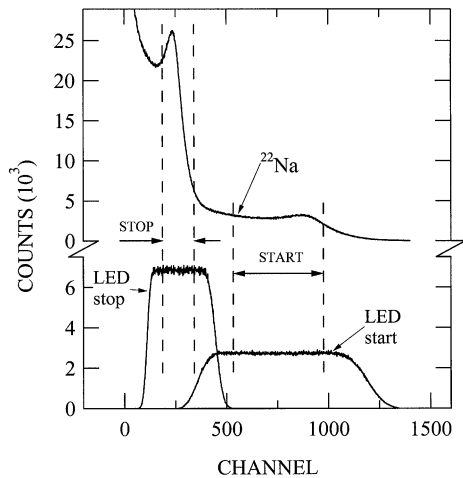


Fig. 4. The distributions of the LED pulses in the start and stop detectors compared to the spectrum due to  $\gamma$ -quanta from a  $^{22}\text{Na}$  source. The dashed lines mark typical (45%) energy windows used in a positron lifetime measurement. The flat regions of the LED spectra have to extend outside the energy windows to enable stable operation in varying ambient conditions.

The reference peak created with the present system is shown in Fig. 5. The FWHM is 210 ps with 45% energy windows set as in a usual positron lifetime measurement (see Fig. 4). The FWHM was found to depend on the driving voltage of the LED so that the narrowest peak was obtained with lowest voltages. This means that the optical fibers should be mounted as close to the LED as possible. The shape of the reference peak is nearly Gaussian over 6 decades as seen in Fig. 5. When a  $^{22}\text{Na}$  source is present in the setup, pulse pile-up causes tails in the reference peak near the background level (see Fig. 2). Due to the small fraction of the pile-up events their effect on the accuracy of centroid determination in the stabilization procedure is, however, negligible. Of course, the lifetime spectrum has to be located far enough outside the distorted region to prevent pulse pile-up events from being taken into the actual spectrum.

The statistical accuracy  $\Delta\text{COM}$  of the centroid of a Gaussian peak is related to the standard deviation  $\sigma$  and the number of counts  $N$  in the peak by  $\Delta\text{COM} = \sigma/\sqrt{N}$ . Thus, with increasing LED-frequency the time needed for a reliable

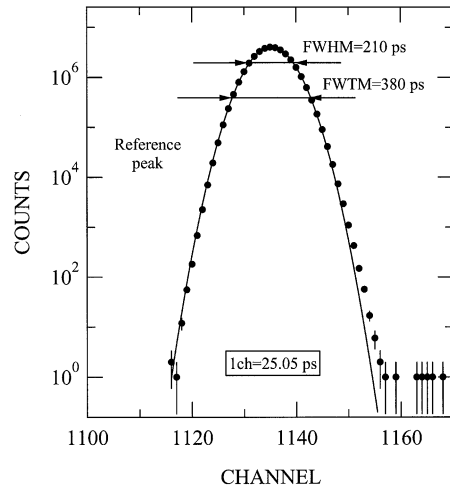


Fig. 5. The reference peak obtained with only LED pulses (no  $\gamma$ -source present). The solid line is a Gaussian fit to the data.

detection of the peak position decreases which, in principle, enables the correction of even the fastest drifts. However, with increasing LED frequency also the current in the photomultiplier tube increases, which results in the degradation of the gain of the tube. Manufacturers of photomultipliers typically recommend limiting the average anode current below  $10\ \mu\text{A}$  if long-term stability is required [10]. With typical pulse height levels, this corresponds to a reference peak frequency of about 10 kHz. With the present apparatus, the accuracy of the reference peak position after a 1-min acquisition with this frequency is 0.12 ps (FWHM = 210 ps).

If a higher accuracy is needed, the flashing frequency can be increased without detrimental effects by lowering the supply voltage over the photomultiplier tubes and using fast preamplifiers [11,12]. With a preamplifier gain of 20 the reference peak frequency can be increased even up to 200 kHz. This leads to an accuracy of 0.026 ps after a 1-min collection (reference peak FWHM = 210 ps). This accuracy can be compared to that achievable in the stabilization scheme presented by Crisp et al. [2]. They base the stabilization on the symmetrical lifetime spectrum acquired by using both detectors to observe both  $\gamma$ -quanta (511 keV and 1.28 MeV). A typical count

rate in the symmetrical spectrum is of the order of 200 counts 1/s. With such a low count rate the accuracy of the centroid achievable in 1 min is about 1 ps. Thus, with fast preamplifiers the external reference peak would enable one to improve the accuracy of stabilization by a factor of about 40 (from 1 to 0.026 ps) compared to stabilization based on the lifetime spectrum itself.

#### 4. Test results

##### 4.1. Time scale of drifts in a positron lifetime spectrometer

To find a reasonable LED flashing frequency we studied the time scale of the drifts with the apparatus presented in the previous section. We used the maximum flashing frequency of 60 kHz which the Ortec 919 MCA can handle. Spectra were acquired and Gaussian functions were fitted at 2.8 s intervals with 1.0 s spent for collection and 1.8 s for analysis and saving. In the main panel of Fig. 6 we show the averaged peak positions calculated from five successive spectra, i.e. each point represents a time of 14 s. During the 45-min-observation period the drift of the peak is clearly observable. The magnitude of the drift is 5 ps and the direction of the peak movement changes five times. The rate of the drift is 0.5 ps in a minute at maximum.

The insert in Fig. 6 shows the first 300 s of the data with each point corresponding to a time of 2.8 s. As seen, no clear trend can be detected and the peak positions are random in this short period. The rest of the original data collected in 2.8 s cycles during the whole 45-min time are similar in the sense that the peak positions are randomly distributed around the rather clear drift curve marked with the solid line in the main panel. These data suggest that in a typical fast coincidence apparatus there are no faster drifts than those leading to the clearly observable movements in Fig. 6.

Accurate detection of the fast drifts (maximum rate of the order of 0.5 ps/min) requires a rather high count rate in the reference peak. Without fast preamplifiers, the 60-kHz frequency used in the

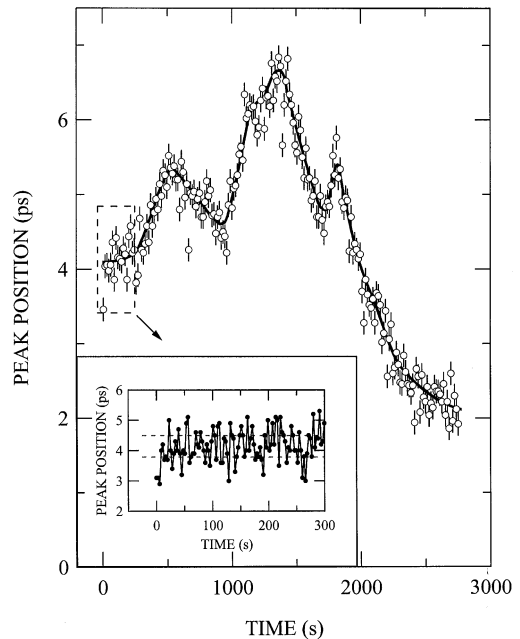


Fig. 6. Reference peak positions in very short measurements. In the main panel each point represents the average centroid of five successive spectra of 2.8 s measurements (14 s total time). In the insert, each point corresponds to a time of 2.8 s. The dashed lines illustrate the theoretical  $2\sigma$  deviation calculated from the FWHM and the number of counts in the peak ( $2\sigma = 0.70$  ps). (The observed STDV 0.54 ps is slightly larger than the ideal STDV 0.35 ps.) The gross features of the data in the main panel show the fastest drifts observed in the spectrometer (the solid line is to guide the eye).

measurement of Fig. 6 is too high for long-term use due to the aging of the PM tubes. In the actual test measurement of our digitally stabilized lifetime spectrometer (see Section 4.2) we made a compromise between the anode current and the accuracy and used a reference peak count rate of 6500 1/s. This leads to an accuracy of 0.14 ps after a 1-min collection time which is sufficient for at least a partial correction of the fast drifts.

An important difference between the point- and Gauss-mode stabilization of the Ortec 919 MCA is that the point mode responds to drifts in real time whereas there is an inherent delay of up to 60 s in the Gauss mode (see Section 2). On the other hand, the corrections in the Gauss mode are more accurate because of the statistics behind them. Hence, considering the rate of drifts illustrated above it is not at all intuitively clear which mode



performs better. We tested the point and Gauss modes by investigating the standard deviation of the stabilized reference peak positions at a frequency of 6500 Hz. The ‘peak preset count’ was chosen low enough such that corrections were carried out once a minute. The result of the test was that there is a factor of two difference in the STDVs with the Gauss mode being better. Hence, we use the Gauss mode in the tests of Section 4.2.

#### 4.2. Performance of a digitally stabilized positron lifetime spectrometer

There are two things to be tested in a stabilized positron lifetime spectrometer. The first is the accuracy with which the reference peak follows the real drifts of the lifetime spectrum. The second is the quality of the stabilization algorithm, i.e. how close the standard deviation of the centroids is to the theoretical minimum ( $\sigma/\sqrt{N}$ ). Both of these properties can be studied simultaneously with the experiment described in the following.

The capability of the reference peak to detect the drifts correctly can be investigated by collecting spectra from the LED pulser and from a  $^{60}\text{Co}$  source at the same time.  $^{60}\text{Co}$  emits two  $\gamma$ -quanta simultaneously. Thus, the drifts in the centroids of the  $^{60}\text{Co}$  spectra represent the drifts of the time zero in real positron lifetime experiments with a  $^{22}\text{Na}$  source.

To test the performance of the digital stabilizer we record the same pulses from the TAC in two different multichannel buffers, one being stabilized and the other not. This can conveniently be done with the Ortec Model 919 MCA consisting of four different buffers, the first of which is digitally stabilized.

The details of the data flow in the experiment can be seen in Fig. 7. The output of the TAC is guided into two buffers MCB1 and MCB2 with the latter signal delayed slightly longer than the dead time of the MCA (delay = 11  $\mu\text{s}$ ). When a pulse from the TAC arrives at the input of MCB1, the microprocessor (MP) makes the connections marked with the thin solid lines. The pulse goes through the stabilizer amplifier (G) to the ADC. Then it is fed to the main memory of MCB1 and the stabilization buffer. The same pulse is next

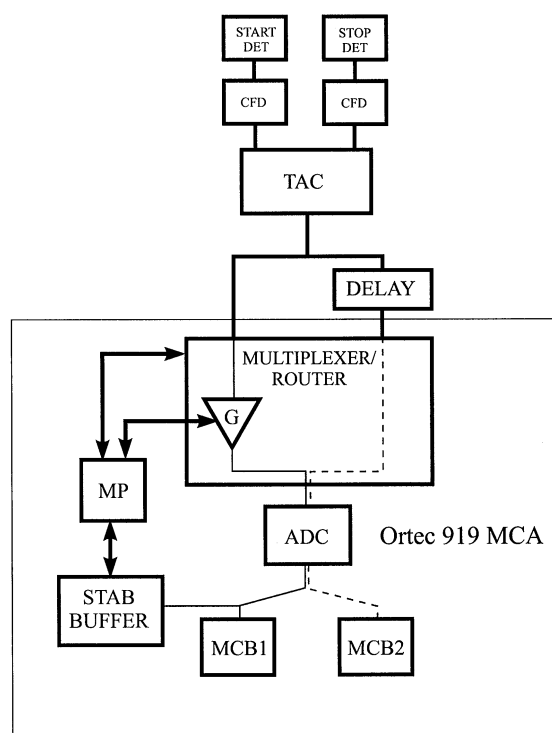


Fig. 7. The experimental setup to test the performance of the reference peak apparatus and the digital stabilizer. Each pulse from the TAC is directed into two multichannel buffers, MCB1 and MCB2, of which only the former uses the digital stabilizer. The pulses coming to MCB2 must be delayed 11  $\mu\text{s}$ .

introduced to the input of MCB2, and is directed straight via the ADC to the memory of MCB2. This chain of events is repeated with the next pulses from the TAC.

When enough counts have accumulated in the stabilization buffer the offset voltage of the stabilizer amplifier is adjusted. No adjustments on the ADC are done. Thus, in this experiment we can detect all the drifts in the chain from the detectors up to the ADC, and the corresponding stabilizer action. If the delay before MCB2 is properly adjusted at minimum, the numbers of counts in MCB1 and MCB2 are equal.

Fig. 8 presents the centroids of the  $^{60}\text{Co}$  peak and the reference peak in a one-week-long measurement in the nonstabilized MCA (MCB 2). Each symbol corresponds to a 20-min measurement. The circles represent the  $^{60}\text{Co}$  peaks and the triangles the LED peaks. The drifts of the two

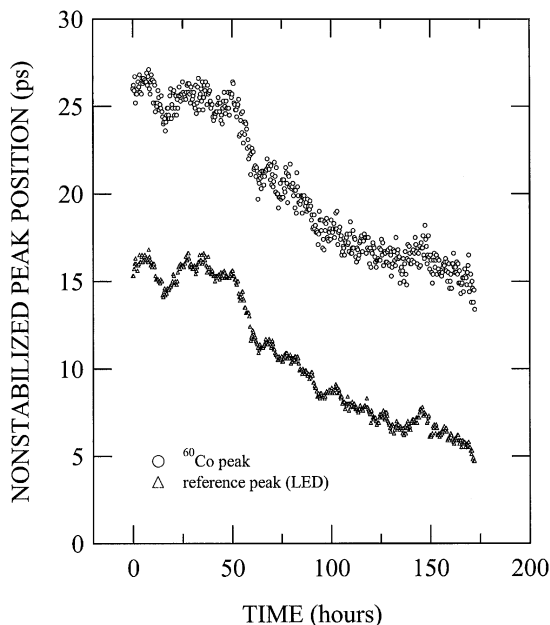


Fig. 8. The centroids of the reference peak and a peak resulting from the two  $\gamma$ -quanta from a  $^{60}\text{Co}$  source in a one-week-long measurement. As seen, the reference peak moves identically with the  $\gamma$ -peak and therefore properly reveals the drifts in the spectrometer.

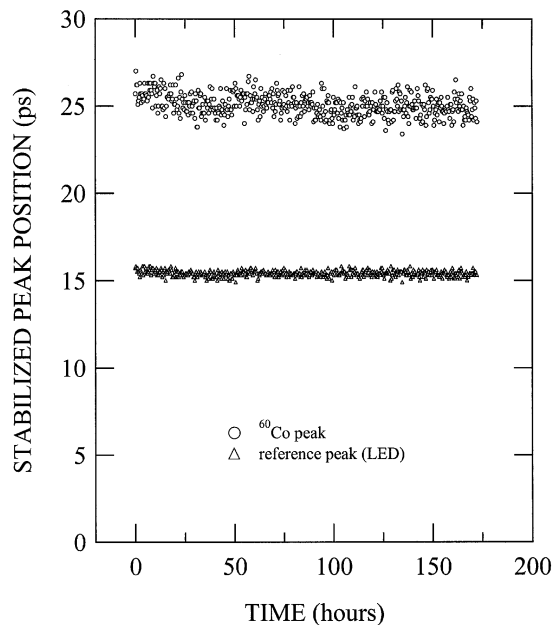


Fig. 9. The centroids of the reference peak and  $^{60}\text{Co}$  peak stabilized with the present system. These data have been collected using the setup presented in Fig. 7 and originate from the same pulses which lead to the data shown in Fig. 8.

peaks are identical. The overall drift of 12 ps in a week is typical for a combination of fast scintillation detectors and commercial timing electronics. The results of stabilization can be seen in Fig. 9 which shows the centroids of the spectra collected in the digitally stabilized MCA (MCB1). As explained, these spectra originate from the same pulses as in Fig. 8. The standard deviation of the reference peak centroids equals 0.17 ps whereas the theoretical STDV is about 0.03 ps. The difference probably results from the inherent delay in the correction (up to 60 s) and the rather large size of the minimum correction (0.125 ps). The centroids of the  $^{60}\text{Co}$  spectra are within 0.6 ps (STDV) from the preset position. The theoretical standard deviation calculated from the FWHM and the number of counts is slightly lower, 0.3 ps. The residual drift in the  $^{60}\text{Co}$  data in Fig. 9 ( $\leq 0.5$  ps) can be attributed to the temperature dependence of the LED-peak position (see Section 3.3).

The results of Fig. 8 indicate that the reference peak follows well those drifts that are present in

the lifetime measurement. Hence, it seems that within the accuracy achieved in this work, one reference peak located close to the lifetime spectrum is a sufficient indicator of the drifts to which the spectrum is exposed to. The data in Fig. 9 show that the apparatus presented in this paper can be used to enhance the quality of positron lifetime data. A further improvement can evidently be attained by using software stabilization and higher reference peak frequencies.

## 5. Summary

We have set up an apparatus with which a highly accurate time reference for fast coincidence systems can be produced. The time reference is based on a flashing LED which feeds light into two optical fibers of different lengths. The other ends of the fibers are mounted near the photocathodes of the photomultipliers. The reference

peak so created can serve as a basis for digital hardware or software stabilization. In test measurements with a positron lifetime spectrometer, drifts of 12 ps in a one-week-long measurement series could be reduced below a level of 0.5 ps with stabilization.

A particular advantage of the system is that a high frequency in the reference peak enables one to detect fast drifts accurately. For example, in a positron lifetime spectrometer, the stabilization can be more accurate by a factor of 40 compared to a system where the stabilization is based on observations of the lifetime spectrum itself. This allows the reduction of even the fastest observed drifts in the system.

## Acknowledgements

We are grateful to K. Fallström (M.Sc.) for many useful discussions.

## References

- [1] A. Dupasquier, A.P. Mills Jr. (Eds.), *Positron Spectroscopy of Solids*, IOS Press, Amsterdam, 1995; K. Saarinen, P. Hautojärvi, C. Corbel, in: M. Stavola (Ed.), *Identification of Defects in Semiconductors*, Academic Press, New York, 1998; R. Krause-Rehberg, H.S. Leipner, *Positron Annihilation in Semiconductors*, Springer, Heidelberg, 1999.
- [2] V.H.C. Crisp, I.K. MacKenzie, R.N. West, *J. Phys. E* 6 (1973) 1192.
- [3] J.P. Teixeira Dias, J. Jesus, C. Lopes Gil, A.P. de Lima, *Proceedings of the Eighth International Conference on Positron Annihilation*, Gent, Belgium, 29 August–3 September 1988, p. 629.
- [4] I.K. MacKenzie, in: W. Brandt, A. Dupasquier (Eds.), *Proceedings of the International School of Physics “Enrico Fermi”, Course LXXXIII*, Varenna, Italy, 14–24 July 1981, p. 220.
- [5] J. Lindskog, L.-G. Svensson, *Nucl. Instr. and Meth.* 133 (1976) 99.
- [6] J.S. Kapustinsky, R.M. DeVries, N.J. DiGiacomo, W.E. Sondheim, J.W. Sunier, H. Coombes, *Nucl. Instr. and Meth. A* 241 (1985) 612.
- [7] EG & G Ortec, *Modular Pulse-Processing Electronics and Semiconductor Radiation Detectors*, 1997.
- [8] G.F. Knoll, *Radiation Detection and Measurement*, 2nd Edition, Wiley, Singapore, 1989.
- [9] P. Horowitz, W. Hill, *The Art of Electronics*, 2nd Edition, Cambridge University Press, New York, 1994.
- [10] Philips Components, *Photomultipliers, Data Handbook*, Book PC04, 1990.
- [11] F. Becvar et al., *Nucl. Instr. and Meth. A* 443 (2000) 557.
- [12] J. Nissilä, unpublished.